Science & Global Security, 23:191–219, 2015

ISSN: 0892-9882 print / 1547-7800 online
DOI: 10.1080/08929882.2015.1087242

Routledge
Taylor & Francis Group

Hypersonic Boost-Glide Weapons

James M. Acton

Nuclear Policy Program, Carnegie Endowment for International Peace, Washington, DC, USA

The United States, Russia and China are developing hypersonic boost-glide vehicles. A simple model of their trajectory is developed by assuming that the vehicle does not oscillate during the transition to equilibrium gliding. This model is used to analyze U.S. Department of Defense data on test flights for the Hypersonic Technology Vehicle-2. This glider's lift-to-drag ratio—a key performance parameter—is estimated to be 2.6. The model is also used to calculate the tactical warning time that a boost-glide attack would afford an adversary. Other aspects of boost-glide weapons' military effectiveness are explored. Approximate calculations suggest that, compared to existing non-nuclear weapons, boost-glide weapons could penetrate more deeply but would be less effective at destroying silos. The distance at which a boost-glide weapon armed with a particle dispersion warhead could destroy a mobile missile is also calculated; it is expected to be significantly larger than for an explosive warhead.

INTRODUCTION

Eighty years after they were first conceived, hypersonic boost-glide weapons are approaching realization. The idea of using a rocket to launch a re-entry vehicle (RV) capable of gliding for extended distances at hypersonic speeds (faster than five times the speed of sound) dates to the 1930s, when it was proposed by the Austrian aeronautical engineer Eugen Sänger.[1] Developments in rocketry following World War II spurred the United States to explore the concept in the late 1950s and early 1960s, culminating in a brief—but extremely well-funded—project to develop the Dyna-Soar, a manned intercontinental glider. Subsequently, in the 1970s and 1980s, the United States revived the concept

Received 19 September 2014; accepted 5 March 2015.
Address correspondence to James M. Acton, Nuclear Policy Program, Carnegie Endowment for International Peace, 1779 Massachusetts Avenue, NW, Washington, DC 20036-2103, USA. E-mail: jacton@ceip.org
Color versions of one or more of the figures in the article can be found online at www.tandfonline.com/gsgs.

with research into rather less ambitious maneuvering re-entry vehicles capable of gliding for hundreds, rather than thousands, of kilometers.[2]

The current American attempt to develop boost-glide weapons dates to 2003 when the administration of George W. Bush initiated a program that became known as Conventional Prompt Global Strike (CPGS) to develop fast, long-range, non-nuclear weapons.[3] The United States has since tested two gliders: the Hypersonic Technology Vehicle-2 (HTV-2) and the Advanced Hypersonic Weapon (AHW).

The HTV-2, which had a planned range of 17,000 km, was tested in April 2010 and August 2011. Both tests were terminated prematurely and this program has now been effectively canceled. Instead, current U.S. efforts are focused on the AHW. According to a 2008 study by the National Research Council of the U.S. National Academies, the AHW would have a range of about 8,000 km and might, therefore, be more accurately described as a non-global Conventional Prompt Global Strike weapon.[4] The AHW was tested successfully in November 2011. A second test, in August 2014, failed because of a booster problem.[5]

Recently, it has become clear that the United States is not the only state with an interest in boost-glide weaponry. In January 2014, Beijing tested a boost-glide system for the first time.[6] A second test, in August 2014 over a planned range of 1,750 km, appears to have ended in failure following a booster problem.[7] There is some evidence that, unlike the United States, China's goal is the delivery of nuclear weapons—although the overall scale and scope of the Chinese program remain extremely murky.[8]

Senior Russian officials have openly indicated an interest in developing an equivalent to Conventional Prompt Global Strike, though none has said unambiguously that Russia is currently doing so.[9] Meanwhile, Pavel Podvig, a well-respected observer of Russian strategic forces, has presented extensive evidence that Russia is currently engaged in a program to flight test a hypersonic maneuverable re-entry vehicle.[10] This work, which has been on-going for more than a decade, was probably initiated for the purpose of developing a nuclear-armed re-entry vehicle capable of penetrating expanded U.S. ballistic missile defenses; whether it is now being applied to the development of a conventionally armed boost-glide system is unclear.

While no particular boost-glide weapon concept is guaranteed to make it to deployment, the general trend is clear: there is resurgence of interest in this technology and, consequently, a significant probability of deployments in the next decade or two.

To assist in understanding the implications of this trend, this article seeks (i) to develop a simple mathematical framework for modeling boost-glide weapons; (ii) to infer the characteristics of cutting-edge systems; and (iii) to start exploring their military effectiveness. The first section (Boost-Glide Physics Redux) presents a minimal model for boost-glide weapons, that is, the

simplest possible mathematical model that captures their essential behavior. This model is then used to analyze the HTV-2 flight tests. The HTV-2 was studied extensively in this article, even though it has effectively been canceled, because it is the only glider about which a significant quantity of technical data has been disclosed. Moreover, it appears to represent the absolute cutting-edge of research and is therefore an indicator of what kind of "high-end" capabilities might eventually be developed. Analysis of the HTV-2 also highlights some of the technical challenges associated with boost-glide weapons in general. The final sections of this article, available in an online supplement, build upon the insights gained in the analysis of the HTV-2 to estimate how much warning time the target state of a boost-glide attack might receive and to explore the the ability of boost-glide weapons to destroy both hard and deeply buried targets and dispersed mobile missiles.

BOOST-GLIDE PHYSICS REDUX

Overview

A glider traveling through the atmosphere experiences a lift force, L, and a drag force, D. As this drag force depletes a glider's internal energy, which has both a kinetic and gravitational potential component, the glider loses both speed and altitude. The distance over which it can stay aloft depends on L/D, that is, the glider's lift-to-drag ratio. Typical L/D values depend on gliding speed, v, which can be conveniently expressed in terms of the Mach number, M, defined as the ratio of a vehicle's speed to the speed of sound.[11]

Subsonic aircraft, for which $M < 1$, generally have lift-to-drag ratios of between 14 and 17.[12] At typical cruising altitudes, they have enough internal energy, a majority of which is gravitational potential energy, to glide for a few hundred kilometers at most. By contrast, when $v^2 \gg 2gh$, where g is the acceleration due to gravity and h is altitude, the internal energy of a glider is dominated by its kinetic component and is much larger than for a subsonic glider, enabling it to glide much further. As derived in Appendix A (available in an online supplement), in this regime, which typically occurs when $M \gtrsim 5$ (depending on altitude), the range of a glider, l_{glide}, is given by

$$l_{\text{glide}} = \frac{r_e}{2}\frac{L}{D}\ln\left(\frac{1}{1-(v_i/v_e)^2}\right), \tag{1}$$

where v_i is the glider's initial speed, $v_e = \sqrt{gr_e}$ is the speed of a satellite in low Earth orbit, and r_e is the radius of the Earth.

The effect on range of increasing a glider's kinetic energy is, however, partially offset by a reduction in its lift-to-drag ratio. Specifically, a widely used relationship connecting the lift-to-drag ratio of an optimally designed glider,

$L/D_{\max}$, to speed is[13]

$$L/D_{\max} = 4 + \frac{12}{M}. \tag{2}$$

This relationship is valid throughout the supersonic regime, when $1 \leq M < 5$, and the hypersonic regime, when $M \geq 5$. It is empirically determined and is not a fundamental law; gliders with a lift-to-drag ratio somewhat higher than $L/D_{\max}$ have been validated in experiments and by computer modeling. Nonetheless, this relationship does help scale the problem and indicates that, at very high speeds, a glider is unlikely to have a lift-to-drag ratio much above 4.

Because the lift-to-drag ratios of hypersonic gliders are relatively modest, they must be boosted to very high initial speeds—a substantial fraction of v_e—to stay aloft for thousands of kilometers. Such extremely high speeds create a range of complex engineering challenges.[14] The hypersonic aerodynamic regime is inherently complex and not nearly as well understood as the subsonic or supersonic regimes. Vast amounts of heat must be dissipated in a way that does not damage the glider's aeroshell. In addition, high deceleration and plasma formation can interfere with the reception of GPS signals, which are used by U.S. boost-glide prototypes and would almost certainly be used by any deployed boost-glide weapon, thus complicating accurate navigation (although plasma formation is much more of a problem with terminally guided ballistic missiles than gliders).[15] Contemporary efforts to develop boost-glide weapons appear largely focused on solving these challenges.

A standard exo-atmospheric gliding trajectory, used by the HTV-2 for example, is shown in Figure 1. The glider is boosted by a large rocket launched in a depressed trajectory. In flight tests, the United States has used modified retired intercontinental ballistic missiles and sea-launched ballistic missiles. Between the end of the boost phase, at time t_1, and the start of re-entry, at time t_2, the glider separates from the launch vehicle. At time t_3, shortly after re-entry, the glider executes a "pull-up" to transition into stable "equilibrium" gliding, in which the glider maintains almost level flight and which begins at time t_4.

Alternatively, it is possible to launch the glider on such a highly depressed trajectory that it never leaves the atmosphere. This strategy appears to have been adopted for the AHW, which the National Research Council describes as "endoatmospheric."[16] In theory, if an endo-atmospheric booster is able to attain horizontal flight at exactly the right altitude it could inject an RV straight into equilibrium gliding without the need for a pull-up. It does not appear, however, as though the AHW test flight involved this kind of direct injection.[17] So, in practice, the HTV-2 and AHW trajectories are probably quite similar after the start of the pull-up.

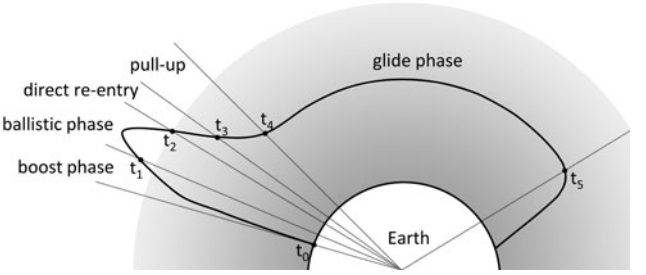

Figure 1: Schematic diagram of the different phases of an exo-atmospheric boost-glide weapon's trajectory. The labels, t_n, indicate the time at which each phase ends. For clarity, radial distances are exaggerated relative to tangential distances, making it appear as though the booster's trajectory is lofted, whereas it is actually depressed.

In any case, the key to modeling the exo-atmospheric trajectory correctly is to understand how the glider avoids bouncing off the atmosphere on re-entry. After all, because atmospheric density increases rapidly with decreasing altitude, the lift force experienced by an RV approaching the atmosphere at a shallow angle can increase sufficiently rapidly to send it back out into space.[18] In this case, the RV skips along the atmosphere in a so-called phugoid trajectory. The theory of skip gliders has been studied extensively. However, it appears that they are not currently being pursued within the CPGS program. It is likely that the U.S. Department of Defense has decided to focus on equilibrium gliding because it reduces the maximum heating rate and the maximum mechanical stress on an RV.[19]

One possible way of preventing a glider from skipping off the atmosphere during re-entry is for it to rotate in such a way that it generates minimal lift. Indeed, a schematic diagram of the HTV-2 flight plan released by DARPA clearly shows the glider re-entering the atmosphere with its flat lower surface roughly perpendicular to its direction of travel, i.e., in a low-lift, high-drag configuration that would tend to prevent skipping.[20] The same diagram shows that the HTV-2 then rotates so that its axis and velocity vector are aligned—a low-drag, high-lift configuration suitable for gliding.

If this rotation were to happen rapidly then the glider would not transition smoothly into equilibrium gliding but would follow a rapidly oscillating trajectory.[21] Such oscillations would, as in the case of a skip glider, result from the rapidly increasing density of the atmosphere inducing a lift force that caused the glider to overshoot its equilibrium position. Although these oscillations would eventually decay, it seems likely that the designers of a practical boost-glide vehicle would want them to be as highly damped as possible

(after all, if they have designed the vehicle for equilibrium gliding rather than skip gliding, then it is to avoid precisely this kind of transient behavior). Indeed, the DARPA schematic shows the glider bouncing just once during the pull-up. One potential way to dampen oscillations is to rotate the glider slowly so that the lift force increases gradually.

The remainder of this section develops a minimal model of this trajectory. In keeping with this approach, the trajectory is assumed to contain no oscillations during the pull-up. The result is a relatively simple model that is (largely) analytically tractable and hence easy to scrutinize. Ultimately, of course, it cannot compete for accuracy with more complex models that must be solved numerically. However, it is hoped that, by elucidating the basic design considerations of the HTV-2, this article will aid efforts by other non-governmental researchers to develop a more complex and accurate model.

Mathematical Formalism

The trajectory of an RV of mass m can, in two-dimensions, be characterized by its speed, v, and path angle, θ, at any point. As shown in Figure 2, θ is the angle between an RV's velocity vector and the local horizontal. By definition, $\theta > 0$ when the velocity vector is below the horizontal (i.e., the RV is traveling downwards). In addition to gravity, the RV experiences two forces due to interactions with the atmosphere: a drag force $D = C_D A \rho v^2/2$, which acts in the opposite direction to its velocity, and lift force $L = C_L A \rho v^2/2$, which acts perpendicular to its velocity, where C_D and C_L are the coefficients of drag and lift, A is the cross-sectional frontal area of the RV, and ρ is the density of the atmosphere. C_D, C_L, and A all depend on the glider's angle of attack, that is, the angle between its long axis and the velocity vector.

In developing a simple mathematical model, the glider is treated as a point-like particle (which involves assuming *inter alia* that its center of mass and center of pressure are the same) with a ballistic coefficient of $\beta = m/C_D A$ and a lift-to-drag ratio of L/D. Both these quantities are allowed to vary along the trajectory as the angle of attack changes. Assuming that the Earth is a perfectly spherical, non-rotating body, the relevant equations of motion are[22]

$$-\frac{\mathrm{d}v}{\mathrm{d}t} = -g\sin\theta + \frac{\rho}{2\beta}v^2 \tag{3}$$

$$\frac{v}{\cos\theta}\frac{\mathrm{d}\theta}{\mathrm{d}t} = g - \frac{v^2}{r} - \frac{\rho}{2\beta\cos\theta}\frac{L}{D}v^2, \tag{4}$$

where t is time and r is the distance of the RV from the center of the Earth. Because any changes in r are very small compared to $r_e = 6{,}400\,\mathrm{km}$, it is standard practice to treat $r = r_e$ and $g = 9.8\,\mathrm{ms}^{-2}$ as constants.

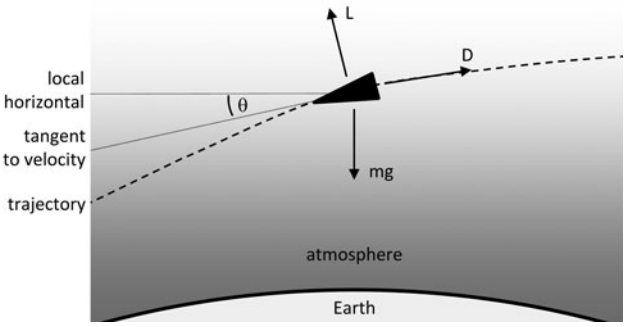

Figure 2: Schematic diagram illustrating the forces acting on a re-entry vehicle traveling through the atmosphere. Note that the angle θ, between the vehicle's velocity vector and the local horizontal, is positive when the vehicle is traveling downwards. Other quantities are defined in the main text. (Not drawn to scale.)

The downrange distance traveled by the RV, x, and its altitude above the Earth's surface, h, are also of interest. The former is related to v and θ by

$$\frac{\mathrm{d}x}{\mathrm{d}t} = v\cos\theta, \tag{5}$$

whereas the latter is given by

$$\frac{\mathrm{d}h}{\mathrm{d}t} = -v\sin\theta. \tag{6}$$

In order to solve these equations, it is necessary to model the variation of atmospheric density with altitude. The relationship between density and altitude can conveniently be expressed as

$$\rho = \rho_0\,\mathrm{e}^{-h/H}, \tag{7}$$

where $\rho_0 = 1.23\,\mathrm{kg\,m^{-3}}$ is atmospheric density at sea level and H, which is a function of h, is the so-called scale height of the atmosphere. In order to make analytic progress, however, it is necessary to take H as a constant (which is physically equivalent to assuming the atmosphere is isothermal). For $30\,\mathrm{km} < h < 100\,\mathrm{km}$, the relevant altitude range for boost-glide vehicles, $\rho_0 = 1.46\,\mathrm{kg\,m^{-3}}$ and $H = 6{,}970\,\mathrm{m}$ yield the best fit with data from the 1976 U.S. standard atmosphere.[23] Using this assumption, it is possible to develop an approximate analytic solution to Eq. (3) and Eq. (4) by breaking the trajectory down into a series of phases, as shown in Figure 1. The variables t, θ, v, x, and h at the end of phase n are given by t_n, θ_n, v_n, x_n, and h_n respectively. The phases are as follows:

Phase 1: Boost phase.

The rocket is launched at $t_0 = 0, x_0 = 0, h_0 = 0, \theta_0 = -90^\circ$ and $v_0 = 0$. Burnout occurs at the end of this phase.

Phase 2: Exo-atmospheric phase.

In this phase, atmospheric forces on the RV are neglected. The trajectory in this phase is ballistic unless the RV is equipped with thrusters that it can use to re-enter the atmosphere sooner than it would otherwise have done.

Phase 3: Direct re-entry.

When the RV reaches an altitude h_2, atmospheric forces can no longer be neglected and the RV starts to decelerate rapidly. It is assumed that, during this phase, the RV is at a large angle of attack, i.e., its flat lower surface is exposed to the atmosphere, resulting in a large drag force and minimal lift. During this phase, the ballistic coefficient is assumed to be a constant, β_S (where the subscript is meant to imply that β is "small") and the lift-to-drag ratio is taken as zero. Numerical simulations of this kind of "direct re-entry" indicate that for $\theta_2 > 5^\circ$, it is a good approximation to treat θ as a constant.[24] If it is further assumed that gravity can be neglected relative to drag then standard analytic solutions exist. These solutions are summarized in Table 1 and their derivation is presented briefly in Appendix A.

Phase 4: Pull-up.

In this phase, it is assumed that the RV gradually rotates into its high-lift, low-drag orientation, causing θ to decrease. For modeling purposes, it is assumed that there are no oscillations during the pull-up. Approximate solutions are derived in the following section and are also included in Table 1.

Phase 5. Equilibrium gliding.

Once $\theta \approx 0$, equilibrium gliding is established. In this phase the ballistic coefficient is denoted by β_L (where the subscript is meant to suggest that β is "large") and the lift-to-drag ratio is L/D. Both L/D and β_L are assumed to be constant during gliding. At the end of this phase, when the glider is a distance x_5 downrange and close to the target, it uses its thrusters to exit the glide and impact on the target. Under the assumptions that $\theta \ll 1$ rad, $\mathrm{d}\theta/\mathrm{d}t \approx 0$, and $g\sin\theta \ll \mathrm{d}v/\mathrm{d}t$, standard analytic solutions, which are summarized in Table 1 and derived in Appendix A, can be obtained.

Pull-up Phase

At time, t_3, the RV starts to execute a pull-up to enable the transition from direct re-entry, when $\theta = \theta_2$, to equilibrium gliding, when $\theta \simeq 0$. The pull-up

Table 1: Equations describing the trajectory of a hypersonic glider during each of its three phases of endo-atmospheric flight. Quantities not defined in the table have already been defined in the main text.

	Phase 2: Direct re-entry	**Phase 3: Pull-up**	**Phase 4: Equilibrium gliding**
v and h	$v = v_2\,\mathrm{e}^{\delta}\exp\left(-\dfrac{H\rho_0}{2\beta_S\sin\theta_2}\mathrm{e}^{-h/H}\right)$	$h_3 - h = R\dfrac{L}{D}\left[\theta_2\left(\dfrac{v_3 - v}{v_3}\right) - \dfrac{1}{2}\dfrac{L}{D}\left(1 + \dfrac{R}{r_e} - \dfrac{gR}{v_3^2}\right)\left(\dfrac{v_3 - v}{v_3}\right)^2\right]$	$h = H\ln\left(\dfrac{\rho_0 r_e}{2\beta_L}\dfrac{L}{D}\dfrac{v^2}{v_e^2 - v^2}\right)$
θ and v	$\theta = \theta_2$	$\theta_2 - \theta = \dfrac{L}{D}\left(1 + \dfrac{R}{r_e} - \dfrac{gR}{v_3^2}\right)\dfrac{v_3 - v}{v_3}$	$\sin\theta = 2\left[\dfrac{r_e}{H}\dfrac{L}{D}\left(\dfrac{v}{v_e}\right)^2\right]^{-1}$
t and v or h	$t - t_2 = \dfrac{h_2 - h}{v_2\mathrm{e}^{\delta}\sin\theta_2} + \dfrac{H}{v_2\mathrm{e}^{\delta}\sin\theta_2}\displaystyle\sum_{n=1}^{\infty}\dfrac{\delta^n}{n\cdot n!}\left(\mathrm{e}^{-n(h-h_2)/H} - 1\right)$	$v = v_3\left(1 - \dfrac{D}{L}\dfrac{v_3\,(t - t_3)}{R}\right)$	$\dfrac{v}{v_e} = \dfrac{\exp\left[-2\frac{D}{L}\frac{g}{v_e}(t - t_4)\right] - \Gamma_4}{\exp\left[-2\frac{D}{L}\frac{g}{v_e}(t - t_4)\right] + \Gamma_4}$
x and t or h	$h_2 - h = (x - x_2)\tan\theta_2$	$x - x_3 = v_3\left[(t - t_3) - \dfrac{D}{L}\dfrac{v_3\,(t - t_3)^2}{2R}\right]$	$x - x_4 = -v_e(t - t_4) + r_e\dfrac{L}{D}\ln\left(\dfrac{1 + \Gamma_4}{\exp\left[-2\frac{D}{L}\frac{g}{v_e}(t - t_4)\right] + \Gamma_4}\right)$
Definitions	$\delta = \dfrac{H\rho_0}{2\beta_S\sin\theta_2}\mathrm{e}^{-h_2/H}$	$R = \dfrac{2\beta_L}{\rho(h_4)}\dfrac{D}{L}$	$\Gamma_4 = \dfrac{1 - v_4/v_e}{1 + v_4/v_e}$

is the phase of motion that is least susceptible to an analytic treatment and, in contrast to the cases of equilibrium gliding and direct re-entry, relatively little attention has been paid to it in the open literature. Nonetheless, if the goal is to analyze empirical data, it is necessary to model the pull-up. Fortunately, because the pull-up represents only a relatively small fraction of the total trajectory and the speed change during the pull-up is relatively small, even a fairly crude model is likely to be adequate for current purposes. (That said, there is little question that analysis of the pull-up would benefit from a numerical treatment).

Mathematically, the oscillations that generally accompany the transition to equilibrium gliding are induced by the third term of the right-side of Eq. (4). Here it is assumed that, in order to dampen them, the glider is gradually rotated during the pull-up. If this rotation, which increases the ballistic coefficient from β_S to β_L, can be timed so that the ratio ρ/β remains constant then the decrease in drag precisely cancels out the rapid increase in density. Because the estimate for β_L obtained in the next section is more reliable than the estimate for β_S, ρ/β is set to $\rho(h_4)/\beta_L$ in constructing the mathematical model of the pull-up. Nonetheless, the assumption that ρ/β is constant obviously implies that

$$\frac{\rho(h_3)}{\beta_S} = \frac{\rho(h_4)}{\beta_L}. \tag{8}$$

Even if ρ/β remains constant, oscillations may still occur because the rotation also causes the glider's lift-to-drag ratio to increase. In the absence of detailed information about the design of a glider, it is not possible to determine how this ratio varies during the pull-up. Moreover, if the lift-to-drag ratio is not a constant, the equations of motion become analytically intractable. Consequently, in keeping with the goal of obtaining a non-oscillatory trajectory, the lift-to-drag ratio is simply taken as the constant L/D during the pull-up. If it is further assumed that $\theta \ll 1$ rad, throughout the pull-up and that the gravitational force is small compared to drag then Eq. (3) and Eq. (4) become

$$\frac{\mathrm{d}v}{\mathrm{d}t} = -\frac{\rho(h_4)}{2\beta_L}v^2 \tag{9}$$

and

$$v\frac{\mathrm{d}\theta}{\mathrm{d}t} = g - \frac{v^2}{r_e} - \frac{\rho(h_4)}{2\beta_L}\frac{L}{D}v^2. \tag{10}$$

Special case: High-speed solution

In finding approximate solutions to these equations, it is instructive, in the first instance, to consider the scenario where the pull-up takes place at speeds comparable to v_e. In this case, the first two terms on the right-hand

side of Eq. (10) cancel out. Then dividing Eq. (9) by Eq. (10) and noting that $\theta_3 = \theta_2$ (because the path angle is assumed to remain constant during the direct re-entry phase), it is straightforward to show that

$$v = v_3 \mathrm{e}^{-\frac{D}{L}(\theta_2 - \theta)}. \tag{11}$$

Because the underlying equations of motion, Eq. (9) and Eq. (10), are only valid when both θ_2 and θ are small, then $\theta_2 - \theta$ must also be small. In this case, Eq. (11) is equivalent to

$$\frac{v}{v_3} = 1 - \frac{D}{L}(\theta_2 - \theta). \tag{12}$$

Equation (11) was derived in the National Research Council study on CPGS by assuming that the glider's trajectory during the pull-up is a circular arc.[25] The framework presented here allows this assumption to be simply proved (as well as revealing that it is only valid when the pull-up takes place at speeds close to v_e). Specifically, it is now convenient to define a new length-scale, R, such that

$$R = \frac{2\beta_L}{\rho(h_4)} \frac{D}{L}. \tag{13}$$

Using this definition, Eq. (10) can be re-expressed as

$$\frac{\mathrm{d}\theta}{\mathrm{dt}} = -\frac{v}{R}. \tag{14}$$

Noting that $\mathrm{d}\theta/\mathrm{d}t < 0$, this result shows that the pull-up at high speeds is indeed the arc of a circle with radius R.

The dependence of θ on t can be found by combining Eq. (12) and Eq. (14) and again invoking the small angle approximation to yield

$$\theta = \theta_2 - \frac{v_3 (t - t_3)}{R}. \tag{15}$$

Within the same approximation scheme, it also follows from Eq. (9) that

$$v = v_3 \left(1 - \frac{D}{L} \frac{v_3 (t - t_3)}{R}\right). \tag{16}$$

This result and Eq. (5) enable the downrange distance traveled during the pull-up to be shown to be

$$x - x_3 = v_3 \left[(t - t_3) - \frac{D}{L} \frac{v_3 (t - t_3)^2}{2R}\right]. \tag{17}$$

Finally, because the trajectory of the RV at high speeds is a circular arc, its change in altitude is given by $h_3 - h = R(\cos\theta - \cos\theta_2)$. Using the small angle

approximation and Eq. (12), this expression becomes

$$h_3 - h = R\frac{L}{D}\left[\theta_2\left(\frac{v_3 - v}{v_3}\right) - \frac{1}{2}\frac{L}{D}\left(\frac{v_3 - v}{v_3}\right)^2\right]. \tag{18}$$

General solution.

If $v \not\sim v_e$ during the pull-up, Eq. (12), Eq. (15) and Eq. (18) cease to be valid, although Eq. (16) and Eq. (17) do remain valid at any speed. It is possible, however, to obtain a more general analytic solution that is valid at any speed. Specifically, the dependence of θ on v can be found by dividing Eq. (9) by Eq. (10) to yield a differential equation with the solution

$$\theta_2 - \theta = \frac{L}{D}\left[\frac{gR}{2}\left(\frac{1}{v_3^2} - \frac{1}{v^2}\right) + \left(\frac{R}{r_e} + 1\right)\ln\left(\frac{v_3}{v}\right)\right]. \tag{19}$$

Because this result is only valid when $\theta_2 - \theta$ is small, then the fractional change in speed during the pull-up must also be small. In this case, linearizing (19) in the small parameter $(v_3 - v)/v_3$ gives

$$\theta_2 - \theta = \frac{L}{D}\left(1 + \frac{R}{r_e} - \frac{gR}{v_3^2}\right)\frac{v_3 - v}{v_3}. \tag{20}$$

A useful check on the algebra is to note that in the high speed limit, when $v \sim v_e$ throughout the pull-up, Eq. (6) becomes identical to Eq. (12).

The change in altitude during the pull-up can be found by substituting Eq. (20) into Eq. (6), employing the small angle approximation, integrating and linearizing to give

$$h_3 - h = R\frac{L}{D}\left[\theta_2\left(\frac{v_3 - v}{v_3}\right) - \frac{1}{2}\frac{L}{D}\left(1 + \frac{R}{r_e} - \frac{gR}{v_3^2}\right)\left(\frac{v_3 - v}{v_3}\right)^2\right]. \tag{21}$$

Once again, the fact that, in the high speed limit, this result becomes equivalent to Eq. (18) provides confidence in the derivation.

MODELING THE HTV-2 TEST FLIGHTS

The HTV-2 flight test program provides an opportunity to apply this model. Specifically, there is enough quantitative data to estimate certain properties of the glider including, most importantly, its lift-to-drag ratio. Moreover, because not all of the available data needs to be used in estimating the model's parameters, its fidelity can be tested by comparing its output to the remaining data points.

When the HTV-2 test program was initiated, flights along two different trajectories, called "A" and "B", were planned.[26] Each route started from

Vandenberg Air Force Base in California and the planned impact point was 7,800 km away in the Pacific Ocean near Illeginni Island, which is part of Kwajalein Atoll in the Republic of the Marshall Islands and lies approximately south-west of the launch site. The A route was a more-or-less straight line between these locations. The B route, which was intended to test the glider's midcourse maneuverability, was to involve the glider first heading almost due west before turning to approach the target from the north.

The first test flight, which took place on 22 April 2010 along the A route, was terminated prematurely after the vehicle began to rotate uncontrollably. As a result, the A route was also used for the second flight test on 11 August 2011. Again, this test was terminated early after the glider's aeroshell was damaged by heating.[27] No more HTV-2 flight tests have taken place since then so the B route has never been attempted.

Quantitative information about the test flights is available from five sources:

- The *Environmental Assessment for Hypersonic Technology Vehicle 2 Flight Tests*, which was prepared by the Space and Missile Systems Center and published in 2009, gives a range of altitudes at which the HTV-2 was to start its glide (h_4) and, more importantly, a single altitude at which it was to leave a gliding trajectory to approach the target (h_5).[28]
- A presentation given by a DARPA employee at the National Institute of Aerospace on 17 June 2009 contains a detailed map of both the A and B trajectories on which various parameters are marked, including the total endo-atmospheric flight time ($t_5 - t_2$), and the speed (v_2) and path angle (θ_2) of the glider at the "pierce point" (the point at which the RV re-enters the atmosphere).[29] The map also states the transverse distance that was to have been flown during the B flight. The relevant picture is reproduced here in Figure 3.
- In April 2010, the website of *Aviation Week* published a second map, similar to that shown in Figure 3, which was reportedly included in a presentation given by a senior DARPA official in December 2009.[30] On this map, arrows along the A and B trajectories indicate the time after launch at which the RV re-enters the atmosphere (t_2) and begins to glide (t_4). The locations of the arrows also allow the distances traveled between re-entry and the end of the pull-up ($x_4 - x_2$), and between re-entry and the end of the glide phase ($x_5 - x_2$) to be estimated—although such estimates have large associated errors because the positions of the arrows appear to be approximate.
- According to the DARPA website, "139 seconds of Mach 22 to Mach 17 aerodynamic data" was collected during the 2010 test.[31] This statement implies

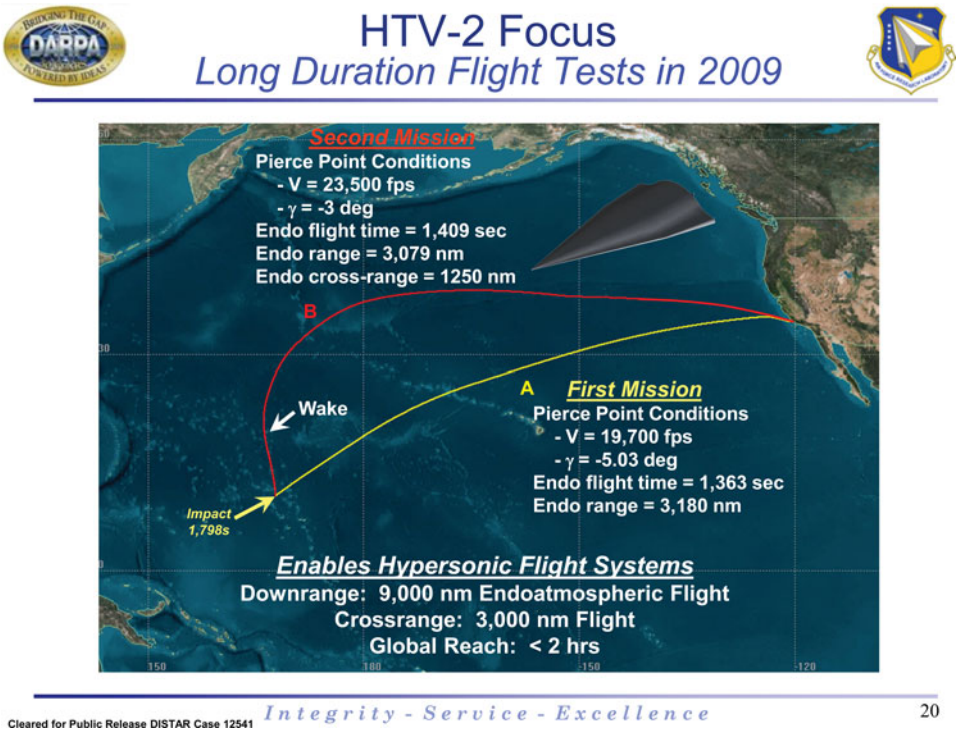

Figure 3: Map from a presentation given by a DARPA employee in June 2009 showing the flight paths for the planned HTV-2 test flights, along with some data about those flights. Note that γ and $-V$, as used in the figure, appear to be equivalent to θ and v respectively, as used in this article.

that at time $t_i = t_2 + 139\,\mathrm{s}$, the vehicle's speed, v_i, was $17 v_s(h_i)$, where $v_s(h)$ is the speed of sound at altitude h, and h_i was the vehicle's altitude at $t = t_i$.

- *Notifications to Mariners*, provided ahead of each of the tests, provide co-ordinates for the drop zones of each of the booster rocket's stages.[32] As described further in the companion article by David Wright (in this issue), these data are consistent with atmospheric re-entry taking place at $h_2 = 100\,\mathrm{km}$, which is a common definition of the altitude of the pierce point. That said, the uncertainty in h_2 must be regarded as significant.

A Flight

All the available data about the A flight is summarized in Table 2. By fitting the model set out in Table 1 to this data, the lift-to-drag ratio and other characteristics of the HTV-2 can be estimated.

The details of the fitting process, which involves solving a set of ordinary, non-linear, simultaneous equations, are described further in Appendix B

Table 2: Summary of known information about the A flight test. The figures in parentheses are subject to significant uncertainties and are not used in fitting the model to the data.

n	t_n (s)	θ_n (deg)	h_n (km)	v_n (ms^{-1})	$x_n - x_2$ (km)
2	435	5.03	100	6,010	0
3		5.03			
4	620		(45.7–76.2)		(1,200)
5	1,798		30.5		5,900
additional information: $v(574\,\text{s}) = 17 v_s(h(574\,\text{s}))$					

(available in an online supplement). Because of the number of unknowns, two of the data in Table 2 do not need to be used in fitting the model. Because only a wide range is available for h_4, this quantity is not used. Likewise, $x_4 - x_2$ is not used since the fractional uncertainty associated with this quantity is particularly large. To enhance numerical stability, the four parameters, L/D, β_S, β_L, and R, are treated as independent in the fitting process (the implications of this assumption are discussed further below).

Selected results of the fitting process—estimates for L/D, β_S, β_L, and R—are shown in Table 3. The fitting process also yields estimates for t_3, h_3, v_3, h_i, h_4, v_4, θ_4, and v_5. From these results, the equations in Table 1 can be used to calculate the glider's speed, altitude, path angle and downrange distance at any time. Using this procedure, the model's predictions for the speed and altitude of the glider as a function of downrange distance are shown in Figure 4.

A number of the model's predictions are consistent with information not used in the fitting process, helping to build confidence in its fidelity. Specifically, the model's predictions for h_4 and $x_4 - x_2$, which are also shown in Table 3, compare well to the values shown in parentheses in Table 2. In addition, the estimate of $\beta_L = 13{,}000\,\text{kg m}^{-2}$ seems reasonable on physical grounds as it is very similar to estimates for the ballistic coefficient of modern ICBM RVs.[33]

Table 3: Estimated parameters for the A test flight, obtained by fitting the model to the data in Table 2.

L/D	2.6
β_S	7.0 kg m^{-2}
β_L	13,000 kg m^{-2}
R	4.9×10^3 km
$x_4 - x_2$	1,100 km
h_4	47 km

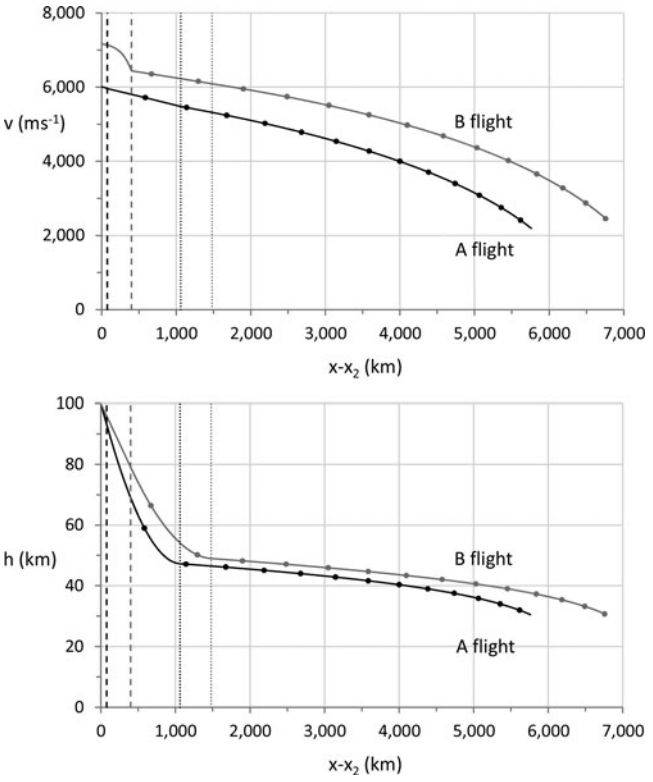

Figure 4: Plots of calculated speed, v (top figure, in ms^{-1}), and altitude, h (bottom figure, in km), against downrange distance from atmospheric re-entry, $x - x_2$ (in km, measured along the trajectory) for the two HTV-2 test flights. The circular markers indicate increments of 100 seconds after re-entry. The dashed lines show the start of the pull-up and the dotted lines show the start of equilibrium gliding.

Another important test of the fidelity of the results is to ascertain how much they change as h_2, which has a bigger uncertainty than any of the other input parameters, is varied. Reassuringly, increasing or decreasing h_2 modestly does not lead to significant changes. For example, increasing h_2 from 100 km to 110 km causes L/D to increase from 2.6 to 2.7. The one exception to this trend is β_S, which increases by a factor of 3 with the same variation in h_2. Meanwhile, decreasing h_2 below 97 km causes β_S to change sign (which is obviously unphysical). The uncertainty in β_S is hardly surprising. The direct re-entry phase in the A flight is estimated to be very short—just 12 seconds. As a result, changes in β_S should affect the trajectory much less than changes in, say, β_L or L/D. The estimate for β_S is, therefore, significantly less reliable than the other values given in Table 3.

Moreover, the estimate for β_S is an order-of-magnitude smaller than might be expected on physical grounds. In the direct re-entry phase, when the HTV-2

is at a large angle of attack, it presents its relatively flat lower surface to the oncoming air. If this surface is modeled as a flat sheet of area A_S at an angle ϕ to the glider's velocity vector then, using a Newtonian approximation, the HTV-2's ballistic coefficient can be estimated as[34]

$$\beta_S = \frac{m}{2A_S \sin^3\phi}. \tag{22}$$

If the HTV-2's lower surface is modeled as an isosceles triangle of height 5 m and width 2 m (so the glider can comfortably enough fit into the fairing of the Minotaur IV Lite launch vehicle[35]) then $A_S = 5\,\mathrm{m}^2$. This value, along with the estimate that $m = 1{,}000\,\mathrm{kg}$ as discussed in the companion article by Wright, implies that $\beta_S > 100\,\mathrm{kg\,m^{-2}}$, a factor of 10 or so bigger than the model's prediction. This failure is probably associated with the simplification of assuming that there is no oscillatory behavior during the pull-up. If the model permitted such behavior, it seems likely that more of the glider's speed would be lost during the pull-up, resulting is less deceleration during the direct re-entry phase and hence a larger value of β_S.

Finally, as noted above, the fitting process treats L/D, β_S, β_L, and R as independent. In fact, according to the model, these four parameters are not independent but should be related by Eq. (8) and Eq. (13). Seeing how closely the results shown in Table 3 adhere to these relationships is another important test. Specifically, using the values of L/D and β_L shown in this table, Eq. (8) predicts that β_S should be $17\,\mathrm{kg\,m^{-2}}$, whereas Eq. (13) predicts that R should be 5.9×10^3 km. This latter value lies within about 20% of the value shown in Table 3, which is respectable given the crudeness of the model. The fractional error associated with β_S is larger, which is not surprising in light of the earlier finding that the estimates of β_S produced by this method are not reliable.

Overall, the available evidence suggests that the model provides a physically reasonable description of the HTV-2's trajectory, except during early endoatmospheric flight, with the consequence that its estimate for β_S should not be considered reliable.

B Flight

Unlike the A flight, the B flight was intended to involve the glider traveling a significant cross-range distance of about 2,300 km.[36] A glider like HTV-2 can move in a transverse direction by banking, that is, rotating about its axis by an angle ψ. Banking in this way creates a force of magnitude $L\sin\psi$ perpendicular to the glider's velocity and causes its trajectory to curve, as shown in Figure 5. Simultaneously, it reduces the lift force on the glider from L to $L\cos\psi$. In fact, within the approximation scheme in which they are valid, the gliding equations shown in Table 1 remain unchanged when the glider banks, except for the replacement of L with $L\cos\psi$.[37]

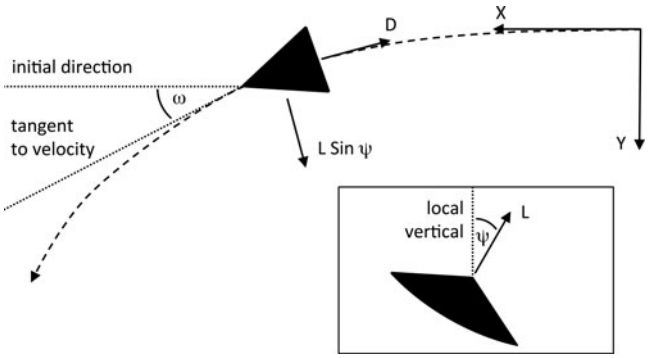

Figure 5: Motion of and forces acting on a glider banking at an angle ψ to the vertical. The main figure shows the view from above. The inset shows a cross section. Other quantities are defined in the text.

Under the assumption that Earth's curvature in the transverse direction can be neglected (that is, the radius of curvature of the glider's trajectory is much smaller than the radius of the Earth), then a new set of coordinates, (X, Y), can be defined, where the X-axis lies parallel to the glider's velocity at the start of the glide phase, as is also shown Figure 5. The glider's position in the X-Y plane at time t is then given by

$$X(t) = \int_{t_4}^{t} \mathrm{d}t' \, v_b\left(t'\right) \cos\left[\omega\left(t'\right)\right], \quad \text{and} \tag{23}$$

$$Y(t) = \int_{t_4}^{t} \mathrm{d}t' \, v_b\left(t'\right) \sin\left[\omega\left(t'\right)\right], \tag{24}$$

where $\omega(t)$ is the angle between the glider's velocity the X-axis, and the speed of the glider while banking, $v_b(t)$, is given by

$$v_b(t) = v_e \frac{\exp\left[-2\frac{D}{L\cos\psi}\frac{g}{v_e}(t-t_4)\right] - \Gamma_4}{\exp\left[-2\frac{D}{L\cos\psi}\frac{g}{v_e}(t-t_4)\right] + \Gamma_4}. \tag{25}$$

As derived in Appendix A, $\omega(t)$ can be shown to be[38]

$$\omega(t) = -\frac{L}{D}\sin\psi \ln\left[\frac{v_b(t)}{v_4}\right]. \tag{26}$$

These results can be used to analyze the B flight and, most importantly, predict the cross-range distance that was to be traversed. This result can then be compared to the figure given by DARPA.

Table 4 shows all the available data about the B flight. Once again, h_4 and $x_4 - x_2$ are not used in fitting the model's parameters to this data. In modeling this flight, it is assumed that the RV does not bank during the pull-up but that,

Table 4: Summary of known data about the B flight test. The figures in parentheses are subject to significant uncertainties and are not used in fitting the model to the data.

n	t_n (s)	θ_n (deg)	h_n (km)	v_n (ms^{-1})	$x_n - x_2$ (km)
2	376	3	100	7,170	0
3		3			
4	606		(45.7–76.2)		(1,900)
5	1,785		30.5		7,200

as soon as gliding starts, it rotates quickly. It is further assumed that L/D and β_L for the B flight are the same as for the A flight.

Using these assumptions, a procedure similar to the one employed to fit the model to the A flight can then be used to extract ψ, β_S, and R as well as $v(x)$ and $h(x)$ for the B trajectory—as shown in Table 5 and Figure 4. It should be noted that the assumption that θ is constant during direct re-entry is questionable for the B flight because $\theta_2 < 5^\circ$. However, given that the direct re-entry phase represents only a relatively small part of the whole trajectory, the consequences of this assumption breaking down should not be too severe.

From Table 5 it can be seen that, once again, the estimated values for h_4 and $x_4 - x_2$ are consistent with the available data. The values of β_S obtained for the A and B flights are also essentially the same, given the significant uncertainty in both estimates.[39] The final check, as before, is to compare the value of R predicted by Eq. (13) to the one found by the fitting process. Here the agreement turns out to be even better than for the A flight. Specifically, Eq. (13) predicts that R should be 7.5×10^3 km, which is in remarkably good agreement with the value shown in Table 5.

This fitting process also estimates the banking angle, ψ, to be 36°. With this information, the shape of the RV's trajectory in the X-Y plane during the glide phase can be evaluated numerically from Eq. (23) and Eq. (24) and is plotted in Figure 6. As can be seen from this figure, the model predicts that, at the end of its flight at time t_5, the glider should have traveled 2,000 km in the Y-direction.

Table 5: Estimated parameters for the B test flight, obtained by fitting the model to the data in Table 4.

ψ	36°
β_S	10 kg m^{-2}
R	8.0×10^3 km
$x_4 - x_2$	1,400 km
h_4	49 km

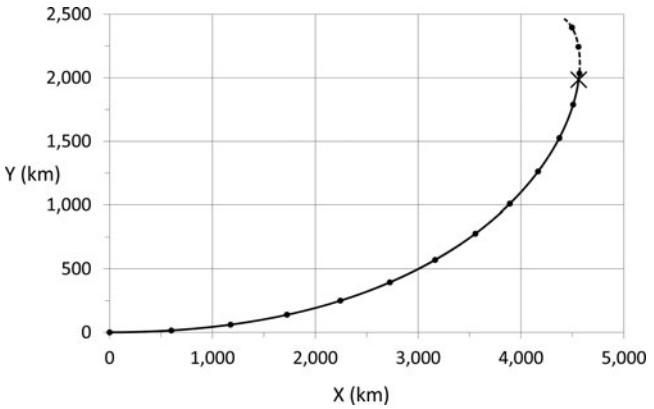

Figure 6: Plot of the calculated trajectory of the B flight in the X-Y plane during the glide phase. The cross shows the planned end of the flight. The dashed line shows the continuation of the trajectory beyond this point. The circular markers indicate increments of 100s. The X- and Y-directions are defined, respectively, to be parallel and perpendicular to the glider's velocity at the start of the glide. Note that the X and Y axes, which are both marked in km, are not drawn to the same scale.

Pleasingly, this estimate is within 15% of the stated value of 2,300 km and provides more evidence that estimates of L/D and β_L are reliable.

More qualitatively, the shape of the trajectory shown in Figure 6 is similar to the published trajectory shown in Figure 3. The former does not, however, "bend back" on itself at the very end as the latter does—although the model can produce this behavior. For example, if the trajectory of the B flight is calculated beyond the planned end time at t_5, shown by the dashed line in Figure 6, then the glider would reverse course.

DISCUSSION

The most important conclusion to be drawn from this analysis is that the HTV-2 has an estimated lift-to-drag ratio of 2.6. This number is similar to the value $L/D = 2.2$ used in the 2008 National Research Council study for sample calculations involving a generic hypersonic glider.[40] It appears, therefore, that the HTV-2 has a lift-to-drag ratio substantially below the theoretical maximum predicted by Eq. (2). The reason is probably that heat management—not aerodynamics—is the limiting factor in determining L/D.

This conclusion may, at first sight, be slightly unexpected. After all, intuitively, one might reason that heat management would become less challenging as L/D increases. Indeed, it follows from Eq. (S.23), in online Appendix A, that the total rate of heat production by a gliding RV is

$$\frac{mgv}{L/D}\left(1-\frac{v^2}{v_e^2}\right), \tag{27}$$

which is inversely proportional to L/D, thus supporting the intuitive conclusion that as drag goes up, heat production also goes up.

However, for thermal protection, what matters is not the total rate of heat production but the rate of heat absorption by the glider (as opposed to absorption by the surrounding air). A key insight into atmospheric re-entry, first understood in the 1950s, is that heat is absorbed more efficiently by an RV with a pointed front end or sharp leading edges.[41] However, thin wings with sharp leading edges are exactly what is needed to increase L/D. It seems likely, therefore, that hypersonic gliders would tend to absorb heat more efficiently as their lift-to-drag ratio increases. The design of the HTV-2, with $L/D \approx 2.6$, appears to represent a compromise between long ranges (which are aided by a high L/D) and a low rate of heat absorption (which requires a low L/D).

Even so, thermal protection remained a problem for the HTV-2. The 2011 test was ended prematurely as a direct result of damage to the glider's aeroshell caused by heating. Thermal protection challenges may also have contributed indirectly to the failure of the 2010 flight test. Specifically, reducing a glider's lift-to-drag ratio to simplify thermal protection requires it to be launched at a higher speed in order not to compromise range. Higher speeds, however, exacerbate the difficulty of control. Indeed, a review into the 2010 flight test concluded that "the most probable cause of the HTV-2 flight anomaly was higher-than-predicted yaw, which coupled into roll thus exceeding the available control capability at the time of the anomaly."[42] Control would presumably have been easier at lower speeds.

Even higher speeds than were planned for the B test would have been needed for the HTV-2 to meet its range goal of 17,000 km. Glide range can be estimated from Eq. (1). It is important to note that this result represents an upper bound for two reasons. First, it assumes that the glider remains aloft until its speed drops to zero. Second, it assumes that the glider travels in a straight line; in practice, maneuvering incurs a range penalty.

The HTV-2 was due to start gliding in the B test at a speed of about $6{,}100\,\mathrm{ms}^{-1}$. Had it simply traveled in a straight line, Eq. (1) predicts that it could have glided for a maximum distance of 7,500 km, implying a total range of 11,700 km. To increase the range to 17,000 km, it follows from Eq. (1) that gliding would need to commence at a speed of $6{,}900\,\mathrm{ms}^{-1}$. In practice, even higher speeds would be required to accommodate cross-range maneuvering and to ensure that the weapon was traveling at a militarily useful speed when it reached the target. However, equilibrium gliding was not successfully achieved in the A test when the aim was to start gliding at "only" $5{,}500\,\mathrm{ms}^{-1}$. It is clear, therefore, that the HTV-2 program was facing significant challenges at the time of its effective cancellation in 2012.

Importantly, lofting the trajectory of the booster to lengthen the exoatmospheric portion of the HTV-2's trajectory appears to be ineffective at increasing range. Specifically, if the the booster is launched on a minimum

energy ballistic trajectory, the glider must pull-up through a much larger angle and loses so much speed while doing so that its glide phase is dramatically shortened. Because of the highly non-linear relationship between glide range and speed, encapsulated in Eq. (1), this effect can more than offset any lengthening of the ballistic portion of the trajectory. For example, in the B flight, the glider was due to start the pull-up at $6{,}440\,\mathrm{ms}^{-1}$. If it were injected into the atmosphere at this speed from a minimum energy ballistic trajectory it would have a path angle of about 30° and, according to Eq. (20), would be slowed to only $2{,}900\,\mathrm{ms}^{-1}$ during the pull-up.[43] So, although the weapon would now cover about 6,700 km before re-entry, it could only travel a maximum of 1,200 km while gliding—shortening the weapon's total range far below what was planned for the B test. Moreover, lengthening the glider's exo-atmopsheric flight at the expense of gliding range would undermine the Department of Defense's argument that gliders would be easily distinguishable from ballistic missiles.

Given that the AHW is now the leading CPGS candidate technology, it would obviously be useful to be able to estimate its lift-to-drag ratio. Unfortunately, there is not enough information to do so. The only public statement on the range of the AHW—8,000 km—appears in the 2008 National Research Council report.[44] Because the AHW has a shorter range than the HTV-2, one might intuitively expect that it also has a lower lift-to-drag ratio. However, this argument is not necessarily correct. The AHW is launched by a less powerful booster than the HTV-2 and so probably travels at significantly slower speeds.[45] If so, it is possible their lift-to-drag ratios are similar.

The analysis of the HTV-2 test flights also raises questions about the survivability of boost-glide weapons. One key argument for developing them is that their speed can defeat advanced air and missile defenses, which are expected to become increasingly widespread over the next few decades. And, to be sure, defending large areas against boost-glide weapons would present very significant challenges (not least because they travel at much lower altitudes than ballistic missiles so would have to be much closer to any given radar to be detectable). There is, however, reason to wonder whether boost-glide weapons could reliably penetrate the sophisticated *point* defenses that advanced states could use to try to defend exactly the high-value targets that CPGS weapons might threaten.[46]

A boost-glide weapon may re-enter the atmosphere at extremely high speeds but it slows as it approaches the target. In both the A and B test flights, it appears that the HTV-2 would have been traveling at between $2{,}000\,\mathrm{ms}^{-1}$ and $2{,}500\,\mathrm{ms}^{-1}$ at the end of its flight. These speeds are characteristic of ballistic missiles with ranges of around 500 km. Even today, such missiles are potentially vulnerable to advanced point defenses and their survivability is likely to be further undermined in the future. To make matters worse, because boost-glide weapons remain in the atmosphere for most of their

trajectory, they cannot be protected by countermeasures such as decoys or chaff.

To be sure, the issue is far from cut and dry. If boost-glide weapons are capable of faster speeds than planned for the HTV-2 test flights, they would be more survivable. Ultimately, however, the survivability of boost-glide weapons might well depend on whether they are capable of executing sufficiently rapid terminal maneuvering to evade interceptors. The United States demonstrated this capability in the 1970s with the Mk-500 "Evader" RV. However, that system was designed to deliver nuclear warheads, which present much less demanding accuracy requirements than non-nuclear ones. Indeed, one potential challenge for boost-glide weapons is that the high accelerations required for evasive maneuvering—measured in tens of *g*—could complicate the reception of GPS signals, potentially undermining accuracy.[47]

Another important issue is whether missile defense interceptors could use the large heat signature of a boost-glide weapon for homing. In particular, one question that deserves further study is whether the U.S. Terminal High Altitude Area Defense (THAAD) system, which uses infra-red homing, could be modified to intercept boost-glide weapons. This question arises because gliders produce much more heat than the ballistic missile RVs that THAAD is intended to counter. However, gliders must be intercepted at lower altitudes than those at which THAAD intercepts typically occur. As a result, heating from atmospheric friction could reduce the efficiency of THAAD's infra-red seeker. Quantitative analysis is needed to determine whether it could still prove effective.[48]

MILITARY EFFECTIVENESS OF BOOST-GLIDE WEAPONS

A discussion of aspects of the military effectiveness of boost-glide weapons is available in an online supplement.

CONCLUSION

From a purely technical perspective, boost-glide weapons would offer certain unique attributes to military planners. Their speed is unmatched by any other kinetic weapon, except for ballistic missiles. And, compared to ballistic missiles, boost-glide weapons have potentially longer ranges, can generally transport a heavier payload over a given range, are capable of midcourse maneuvering, and fly at lower altitudes. Understanding whether these attributes would be likely to provide a significant military advantage and, ultimately, whether the benefits of boost-glide weapons would outweigh their costs and risks raises a complex series of technical and policy questions.[49]

This article, some of which appears in an online supplement, explores some of the technical issues, including the ability of boost-glide weapons to defeat defenses, to deny an adversary tactical warning of an attack, and to destroy mobile targets and hard and deeply buried ones. Given all the uncertainties, there are no simple "yes or no" answers to important questions about boost-glide weapons' military capabilities. In fact, this article's most important contribution may be the new questions that are raised by its findings and, just as importantly, its limitations. At least seven such questions stand out:

- First, what are the characteristics—the lift-to-drag ratio, in particular—of hypersonic gliders other than the HTV-2? Weapon prototypes that are currently being flight tested, including the U.S. Advanced Hypersonic Weapon, the Chinese WU-14 and probable Russian programs, are of obvious interest.
- Second, what limit does thermal protection place on the performance of hypersonic gliders? Difficulties associated with heat management appear to have been fatal to the HTV-2 program. This failure highlights the importance of understanding quantitatively how the challenge of heat management is affected by a glider's speed and lift-to-drag ratio. This, in turn, would help understand what ranges gliders might be able to travel, how far they might be able to maneuver cross-range, and how prompt they could be.
- Third, would a more sophisticated mathematical model of the boost-glide trajectory—of the pull-up, in particular—provide a *qualitatively* new understanding of the physics of boost-glide vehicles? The model set out in this article is a minimal one, simple enough to enable an analytic treatment. While a more complex and realistic model would presumably lead to some quantitative changes in the results presented here, it would be interesting to know whether it would lead to a qualitatively different picture.
- Fourth, would advanced terminal missile defenses be effective at defeating boost-glide weapons? Although this article identifies a series of reasons why intercepting gliders may be easier than intercepting ballistic missiles, no definitive conclusion can be reached because it is unclear whether a glider could execute sufficiently rapid terminal maneuvering to evade interceptors. This question deserves more analysis. Likewise, the challenges of modifying an interceptor missile armed with an infra-red seeker to intercept a glider relatively low in the atmosphere, where heating can be a significant problem for the infra-red sensor, also deserve further consideration.
- Fifth, would boost-glide weapons be vulnerable to countermeasures besides missile defenses? The most obvious example of such a countermeasure is

GPS jamming. Understanding—at a quantitative level—the limitations on weapon accuracy imposed by high-powered GPS jammers and the extent to which they could be mitigated has important policy implications.

- Sixth, what are the costs and benefits of developing early warning sensors designed to detect the heat signal of incoming gliders. In theory, airborne and/or space-based infra-red detectors could be used for this purpose, but more work is needed to understand the trade-offs relative to other detection systems. One particularly interesting question is whether the heat signal of a glider is sufficiently strong to be detected by existing infra-red detection satellites, which are in geostationary orbit, or whether new satellites orbiting at a lower altitude would be required.
- Seventh, and finally, are there militarily important targets that boost-glide weapons are *uniquely* capable of holding at risk? Although weapon effects are discussed in this article, some of the assumptions employed (particularly in the discussion of silo vulnerability) are quite crude and might benefit from being refined. Moreover, to ask whether boost-glide weapons are uniquely capable of threatening some targets is to demand a detailed comparison with other weapon systems and their capabilities.

ACKNOWLEDGMENT

I am indebted to Tom Ehrhard, Richard Garwin, members of Princeton University's Science and Global Security Program and, above all, David Wright for useful conversations and valuable comments on earlier drafts. Of course, the contents of this article remain my own responsibility.

FUNDING

This work was primarily funded by the John D. and Catherine T. MacArthur Foundation, with supplementary support from the William and Flora Hewlett Foundation and the Carnegie Corporation of New York.

SUPPLEMENTAL MATERIAL

Supplemental data for this article can be accessed on the publisher's website.

NOTES AND REFERENCES

1. Robert Godwin, introduction to *Dyna-Soar: Hypersonic Strategic Weapons System*, ed. Godwin (Burlington, ON: Apogee Books, 2003), 7. Sänger subsequently developed the concept theoretically with his wife, the engineer Irene Bredt, under sponsorship of the German Government. See E. Sänger and I. Bredt, *A Rocket Drive*

for Long Range Bombers [Über einen Raketenantrieb für Fernbomber], trans. M. Hamermesh, CGD-32 (Technical Information Branch, Navy Department,[1952]), www.astronautix.com/data/saenger.pdf.

2. For a summary of these efforts see James M. Acton, *Silver Bullet? Asking the Right Questions About Conventional Prompt Global Strike* (Washington, DC: Carnegie Endowment for International Peace, 2013), 37–8, http://carnegieendowment.org/files/cpgs.pdf.
3. For the history of the CPGS program see Amy F. Woolf, *Conventional Prompt Global Strike and Long-Range Ballistic Missiles: Background and Issues*, CRS Report for Congress, R41464 (Congressional Research Service, May 5, 2014). The latest version of this report is available from www.fas.org/sgp/crs/nuke/R41464.pdf.
4. Committee on Conventional Prompt Global Strike Capability, Naval Studies Board, and Division on Engineering and Physical Sciences, the National Research Council of the National Academies, *U.S. Conventional Prompt Global Strike: Issues for 2008 and Beyond* (Washington, DC: National Academies Press, 2008), 115, www.nap.edu/catalog.php?record_id=12061.
5. David Alexander and Andrea Shalal, "Experimental U.S. Hypersonic Weapon Destroyed Seconds After Launch," Reuters, August 25, 2014, http://www.reuters.com/article/2014/08/25/us-usa-military-hypersonic-idUSKBN0GP1ED20140825.
6. "China Confirms Hypersonic Missile Carrier Test," Reuters, January 15, 2014, www.reuters.com/article/2014/01/15/us-china-missile-idUSBREA0E0Z020140115.
7. James Acton, Catherine Dill, and Jeffrey Lewis, "Crashing Glider, Hidden Hotspring: Analyzing China's August 7, 2014 Hypersonic Glider Test," *Arms Control Wonk* (blog), September 3, 2014, http://lewis.armscontrolwonk.com/archive/7443/crashing-glider-hidden-hotspring.
8. Ibid. For more general discussions of Chinese efforts see Acton, *Silver Bullet?*, 100–3; Mark A. Stokes, "China's Quest for Joint Aerospace Power: Concepts and Future Aspirations" in *The Chinese Air Force: Evolving Concepts, Roles, and Capabilities*, eds. Richard P. Hallion, Roger Cliff, and Phillip C. Saunders (Washington, DC: National Defense University Press for the Center for the Study of Chinese Military Affairs, Institute for National Strategic Studies, 2012), 50–5, www.ndu.edu/press/lib/pdf/books/chinese-air-force.pdf; Lora Saalman, "Prompt Global Strike: China and the Spear," Asia Pacific Center for Security Studies, April 2014, http://www.apcss.org/wp-content/uploads/2014/04/APCSS_Saalman_PGS_China_Apr2014.pdf.
9. See, for example, Anatoly Antonov, "Russia Forced to Develop Global Prompt Strike Weapons," *Security Index* 19, (2013): 7; "Russia to Develop Precision Conventional ICBM Option" RIA Novosti, December, 14 2012, http://en.rian.ru/military_news/20121214/178154441.html.
10. Pavel Podvig, "Russian Hypersonic Vehicle—More Dots Added to Project 4202," *Russian Strategic Nuclear Forces* (blog), August 26, 2014, http://russianforces.org/blog/2014/08/russian_hypersonic_vehicle_-_m.shtml and links therein. See also Acton, *Silver Bullet?*, 106–7.
11. The speed of sound is a function of altitude and varies *non*-monotonically from 340 ms^{-1} at sea-level to 275 ms^{-1} at an altitude of 85 km. At higher altitudes, when the wavelength of sound becomes comparable to the mean free path of atmospheric gases, speed of sound ceases to be a valid concept.
12. John D. Anderson, Jr., *Introduction to Flight*, 4th ed. (Boston, MA: McGraw-Hill, 2000), 703.
13. Ibid., 703–4.

14. Acton, *Silver Bullet?*, 59–61.
15. Defense Science Board, *Time Critical Conventional Strike From Strategic Standoff* (Washington, DC: Office of the Under Secretary of Defense for Acquisition, Technology, and Logistics, March 2009), 26–8, www.acq.osd.mil/dsb/reports/ADA498403.pdf; Committee on Conventional Prompt Global Strike Capability, *U.S. Conventional Prompt Global Strike*, 52–3 and 121–3.
16. Committee on Conventional Prompt Global Strike Capability, *U.S. Conventional Prompt Global Strike*, 115.
17. Debra G. Wymer, "Advanced Hypersonic Weapon Flight Test Overview to the Space & Missile Defense Conference," U.S. Army Space and Missile Defense Command/Army Forces Strategic Command, August 14, 2012, 5, http://www.smdc.army.mil/TechCenter/2013/PowerPoint/FINALAHWBrieftoSMDConference081312.pptx.
18. For a quantitative discussion see Frank J. Regan and Satya M. Anandakrishnan, *Dynamics of Atmospheric Re-Entry* (Washington, DC: American Institute of Aeronautics and Astronautics, 1993), 190–2.
19. Alfred J. Eggers, Jr., H. Julian Allen, and Stanford E. Neice, *A Comparative Analysis of the Performance of Long-Range Hypervelocity Vehicles*, Report 1382 (Washington, DC: National Advisory Committee for Aeronautics, [1958]), 12-3, http://ntrs.nasa.gov/archive/nasa/casi.ntrs.nasa.gov/19930092363_1993092363.pdf
20. DARPA, "Falcon HTV-2," www.darpa.mil/Our_Work/TTO/Programs/Falcon_HTV-2.aspx (now available from http://web.archive.org/web/20120205015141/http://www.darpa.mil/Our_Work/TTO/Programs/Falcon_HTV-2.aspx).
21. Dean R. Chapman, *An Approximate Analytical Method for Studying Entry into Planetary Atmospheres*, Technical Note 4276 (Washington, DC: National Advisory Committee for Aeronautics, May 1958), 24, http://naca.central.cranfield.ac.uk/reports/1958/naca-tn-4276.pdf. For a more intuitive presentation, see Carl Gazley, Jr., "Atmospheric Entry" in *Handbook of Astronautical Engineering*, ed. Heinz Hermann Koelle (New York, NY: McGraw-Hill Book Company, 1961), 10-18.
22. Regan and Anandakrishnan, *Dynamics of Atmospheric Re-Entry*, 180–3.
23. National Oceanic and Atmospheric Administration, National Aeronautics and Space Administration, and United States Air Force, *U.S. Standard Atmosphere, 1976*, NOAA-S/T 76-1562 (Washington, DC: U.S. Government Printing Office, October 1976), www.dtic.mil/cgi-bin/GetTRDoc?Location=U2&doc=GetTRDoc.pdf&AD=ADA035728. See also, Regan and Anandakrishnan, *Dynamics of Atmospheric Re-Entry*, 37–8.
24. Gazley, "Atmospheric Entry," 10-10.
25. Committee on Conventional Prompt Global Strike Capability, *U.S. Conventional Prompt Global Strike*, 208.
26. Acquisition Civil/Environmental Engineering, Space and Missile Systems Center, *Environmental Assessment for Hypersonic Technology Vehicle 2 Flight Tests*, April 2009, 16, www.dtic.mil/dtic/tr/fulltext/u2/a544343.pdf.
27. For a more detailed discussion of the test program and its challenges see Acton, *Silver Bullet?*, 40–8 and 59–61.
28. Acquisition Civil/Environmental Engineering, Space and Missile Systems Center, *Environmental Assessment for Hypersonic Technology Vehicle 2 Flight Tests*, 15.
29. Jess Sponable, "Reusable Space Systems: 21st Century Technology Challlenges [Sic]," DARPA, June 17, 2009, 20. No longer available online.

30. Graham Warwick, "DARPA's HTV-2 Didn't Phone Home," *Ares* (blog), *Aviation Week*, April 24, 2010 (now available from http://archive.today/LPwT).
31. "Falcon HTV-2," DARPA.
32. National Geospatial-Intelligence Agency and U.S. Department of Defense, *Notice to Mariners*, no. 18, May 1, 2010, III-1.10, http://msi.nga.mil/MSISite Content/StaticFiles/NAV_PUBS/UNTM/201018/NtM_18-2010.pdf.
33. John R. Harvey and Stefan Michalowski, "Nuclear Weapons Safety: The Case of Trident," *Science & Global Security* 4, (1994): 51; Lisbeth Gronlund and David C. Wright, "Depressed Trajectory SLBMs: A Technical Evaluation and Arms Control Possibilities," *Science & Global Security* 3, (1992): 113. Note these sources use a slightly different definition for β from the one adopted here (mg/C_DA as opposed to m/C_DA).
34. Anderson, *Introduction to Flight*, 696.
35. Acquisition Civil/Environmental Engineering, Space and Missile Systems Center, *Environmental Assessment for Hypersonic Technology Vehicle 2 Flight Tests*, 9.
36. Sponable, "Reusable Space Systems," 20.
37. S. Y. Chen, *The Longitudinal and Lateral Range of Hypersonic Glide Vehicles with Constant Bank Angle*, Memorandum RM-4630-PR (Santa Monica, CA: RAND Corporation, January 1966), 10–1, www.dtic.mil/cgi-bin/GetTRDoc?Location=U2&doc=GetTRDoc.pdf&AD=AD0629124.
38. Ibid.
39. In fact, β_S does not need to be identical for the two flights because the glider may have been due to re-enter the atmosphere in the B flight in a slightly different orientation from the A flight. Nonetheless, it is reassuring that the two estimates are similar, even if they are almost certainly significantly smaller than the true value.
40. Committee on Conventional Prompt Global Strike Capability, *U.S. Conventional Prompt Global Strike*, 206.
41. H. Julian Allen and A. J. Eggers, Jr., *A Study of the Motion and Aerodynamic Heating of Ballistic Missiles Entering the Earth's Atmosphere at High Supersonic Speeds*, Report 1381 (Washington, DC: National Advisory Committee for Aeronautics, 1958), http://ntrs.nasa.gov/archive/nasa/casi.ntrs.nasa.gov/19930091020_1993091020.pdf.
42. DARPA, "DARPA Concludes Review of Falcon HTV-2 Flight Anomaly," Press Release, November 16, 2010, www.darpa.mil/WorkArea/DownloadAsset.aspx?id=2147484134.
43. This calculation is rather approximate because it ignores the direct re-entry phase and because the small angle assumption underlying Eq. (20) is questionable for a path angle of 30°.
44. Committee on Conventional Prompt Global Strike Capability et al., *U.S. Conventional Prompt Global Strike*, 115.
45. U.S. Army Space and Missile Defense Command/Army Forces Strategic Command, *Advanced Hypersonic Weapon Program: Environmental Assessment*, June 2011, 2-2–2-3, www.smdcen.us/pubdocs/files/AHW%20Program%20FEA–30Jun11.pdf
46. Acton, *Silver Bullet?*, 73–7.
47. Defense Science Board, *Time Critical Conventional Strike From Strategic Standoff*, 26–8; Committee on Conventional Prompt Global Strike Capability et al., *U.S. Conventional Prompt Global Strike*, 122.
48. For a discussion of the THAAD seeker's operation in *exo*-atmospheric intercepts see George N. Lewis, "Estimating the Detection Range of a THAAD-Like

Seeker" in He Yingbo and Qiu Yong, "THAAD-Like High Altitude Theater Missile Defense: Strategic Defense Capability and Certain Countermeasures Analysis," *Science & Global Security* 11, (2003): Appendix C, http://scienceandglobalsecurity.org/archive/sgs11yong.pdf.

49. Acton, *Silver Bullet*?